

Impact of Assimilation of Doppler Radial Velocity on a Variational System and on its Forecasts

Fathalla A. Rihan^{a*}, Chris G. Collier^a & Sue P. Ballard^b

^aSchool of Environment and Life Sciences, Peel Building, Salford University, Manchester M5 4WT, UK.

^bMet Office, JCMM, Meteorology Building, Reading University, Berkshire, RG6 6BB, Reading, UK.

An approach to the assimilation of Doppler radar radial winds into a high resolution Numerical Weather Prediction (NWP) model is described. In this paper, we discuss the types of errors which might occur in radar radial winds. A new approach to specifying the radial velocity observation error is proposed based upon the radial gradient of the velocity across the pulse volume. The variation of this error with range is derived for a specific case. The production of "super-observations" for the input to a 3D-Var assimilation system is discussed. Impact of the assimilation of Doppler velocities on the 3D-Var analysis and on the model forecasts, for a case study, is investigated.

1. Introduction

Numerical Weather Prediction (NWP) is considered as an initial-boundary value problem: given an estimate of the present state of the atmosphere, the model simulates (forecasts) its evolution. Specification of proper initial conditions and boundary conditions for the numerical dynamical models is essential in order to have a well-posed problem and subsequently a good forecast model. (A well-posed initial/boundary problem has a unique solution that depends continuously on the initial/boundary conditions.) The goal of *data assimilation* is to construct the best possible *initial* and *boundary* conditions, known as the analysis, from which to integrate the NWP model forward in time.

Assimilation of Doppler radar wind data into atmospheric models has recently received increasing attention due to developments in the use of limited area high resolution numerical models for weather prediction. The models require observations with high spatial and temporal resolution to determine the initial conditions, for which purpose radar data are particularly appealing. However, the resolution of Doppler radar observations is much higher than that of the mesoscale NWP model. Before the assimilation, these data must be preprocessed to be representative of the characteristic scale of the model. To reduce the representativeness error and correspond the data more closely to the model resolutions than do the raw observations, one may spatially interpolate (average) the raw data to generate the so called

super-observations; see Section 4.

Over the last thirty years or so networks of weather radars, providing measurements of radar reflectivity, from which rainfall has been estimated, have been established within operational observing systems. Initially the radars, operating at S-band (10 cm) or C-band (5-6 cm) wavelengths, did not have the capability to measure the motion of the targets (mainly hydrometeors but also insects and birds, and for high power systems, refractive index inhomogeneities) towards or away from the radar site. During the last twenty years or so weather radars having Doppler capability measuring radial motion of the targets have become standard such that now in Europe well over half of the operational radars are Doppler systems (see [2]).

Considerable effort has been, and continues to be, put into the development of nowcasting techniques based upon the extrapolation of radar reflectivity fields aimed at generating forecasts of precipitation up to 3-6 hours ahead (for a review; see [3,10]). Whilst such systems have met with some success, particularly when incorporating wind fields from mesoscale numerical models [5], they are not appropriate for forecasting to longer lead times. Improvements to forecasts for these lead times are now being sought through the assimilation into mesoscale models of radar reflectivity using latent heat nudging methods [15] and variational techniques in which model 'reflectivity' is compared with actual measured reflectivity [22]. More recently Doppler radar radial winds have also been assimilated into NWP models as vertical wind profiles derived from Velocity

*corresponding author F.Rihan@salford.ac.uk

Azimuth Display (VAD) analysis ([1,12]) and using variational techniques (see [23,24]).

In order to assimilate Doppler radial velocity observations, the observation errors which come from several sources are estimated for inclusion in the variational system. In this paper we outline the likely errors in estimates of Doppler radar radial winds, and how they might be represented mathematically. To illustrate the results, we apply the methodology to a case study for data collected using the $3GHz$ radar situated at Chilbolton in southern England (51.14° N and 1.44° W). The large $25m$ antenna affords a beam width of 0.28° , using PPI data² at $300m$ range resolution and 0.25° azimuth resolution. We describe the radial wind and error representation as part of a system for generating simulated data for use in the Met Office variational system. We also investigate the impact of assimilation of Doppler radial velocities and their errors on the variational analysis and on the model forecasts.

1.1. Errors in the determination of Doppler radial velocity

Targets moving away from or towards a radar produce a Doppler shift between the frequency of the transmitted signal (pulse), and the signal reflected from the targets and received back at the radar. However, ambiguities may arise in these measurements due to range folding and velocity aliasing (see [4]). Fortunately procedures have been developed to minimize these problems (see for example [6]).

Other problems remain, namely the existence of data holes (where there are no targets), and irregular coverage, instrumental noise and sampling errors. Various types of interpolation schemes have been used to fill in data holes and poor coverage (see for example [11]), although such schemes are unnecessary when three dimensional assimilation schemes are implemented. However, the impacts of instrumental noise and sampling are more problematic.

May *et al.* (1989) discuss, and assess, a number of techniques used to estimate the Doppler shift in the received signals. The Doppler shift is proportional to the slope of the phase of the autocorrelation function (at zero lag) of the returned signals. An estimator of the shift is the phase at the first lag divided by the value of the lag in time units. This is known as pulse pair processing, and may be improved by averaging more than one value of the phase divided by the lag (poly pulse pair).

An alternative approach is to estimating the

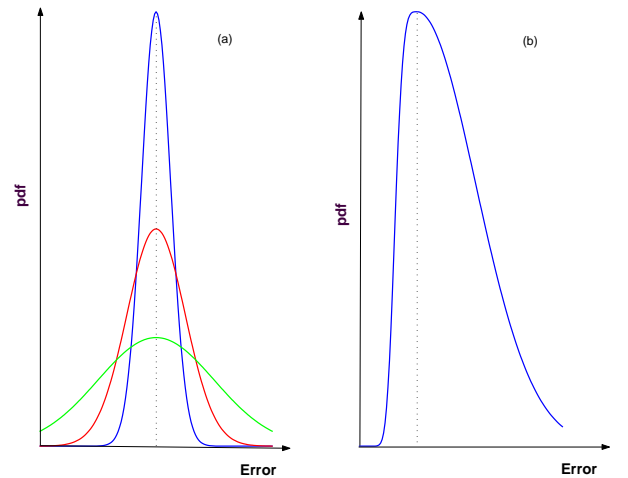


Figure 1. Distribution of wind speed error due to (a) variations of instrumental noise, and (b) strong velocity gradient along the pulse volume at a specific range and azimuth.

Doppler shift directly from the first moment of the Doppler spectra [4] perhaps using a maximum likelihood estimator (similar to a least squares fit) of the logarithmic spectral signal. A further technique is possible based upon the analysis of the power spectrum, its circular convolution and Fast Fourier Transform (FFT) of the same. Interestingly, it was concluded by May *et al.* (1989) that the major limitation to the radar performance is the small-scale variability of the wind along the pulse volume. Therefore there is little to be gained by using complicated algorithms to estimate the Doppler shift. The width of the Doppler spectrum, usually assumed to be Gaussian, determines the correlation time of the signal. Therefore, the error in the radial velocity measurements depends on the strength of the returned signal and the spread or width of the Doppler velocity spectrum which in turn depends mainly on reflectivity and velocity gradients within and across the pulse volume; see [4].

Instrumental errors may be reduced by selecting measurements at range intervals somewhat longer than the radar range gate resolution [8]. For example, [25] selected data every 1 km along each radar beam for a radar having a range gate resolution of 250 m.

Sampling errors depend upon the size of the pulse volume corresponding to each data point. The

²Plan Position Indicator, with constant elevation angle.

Chilbolton radar in central South England has a pulse volume of about 300 m by 0.25 degree, and, even though this is relatively small, even smaller scale wind variability may introduce different sampling errors from measurement point to measurement point. In practice the sampling errors could be weakly correlated from point to point, but only a very small additional error will be introduced if this is ignored. Practically, sampling errors dominate since instrumental errors are usually minimized in operational systems. In the following we outline a system for creating artificial radar radial wind data sets within which different types of error may be included. Figure 1 shows schematics of the impact upon a Gaussian Doppler spectrum of various effects of strong wind shear along the pulse volume, and instrumentally-induced effects. Several of these effects upon the Doppler spectrum may be present in the same radar image, and, in the case of geophysically-induced effects, their magnitude may vary with range and azimuth. The height and size of the pulse volumes will increase with increasing distance from the radar.

This paper is organized as follows: In section 2, we describe a simulation model which is used to analyse actual radial winds. In Section 3, we present a description of the Met Office 3D-Var system for assimilation of Doppler radial winds. In Section 4, we discuss the main steps of preprocessing the Doppler radial data that includes data quality control and super-obbing the very high resolution raw data. We describe the types of errors in radar radial winds and how the radial wind errors may be represented mathematically in Section 5. The proposed methodology is used to derive the variation of the errors with range. Section 6 provides a discussion of assimilation of radial winds in PPI format and observation operator. In Section 7, we investigate the impact of assimilation of radial velocities on the variational analysis and on the forecasts. Conclusion and plans are outlined in Section 8.

2. Comparison of simulated and actual radar winds

Air movement varies over time and space. However, Doppler radar allows the measurement of only one (radial) component of the velocity of the targets at a specific range and azimuth. Since we only take the data from a single radar in the present study rather than simultaneous measurements with three Doppler radars, we are forced to make a simplifying assumption to the structure of the observed wind

field during the creation of Doppler products.

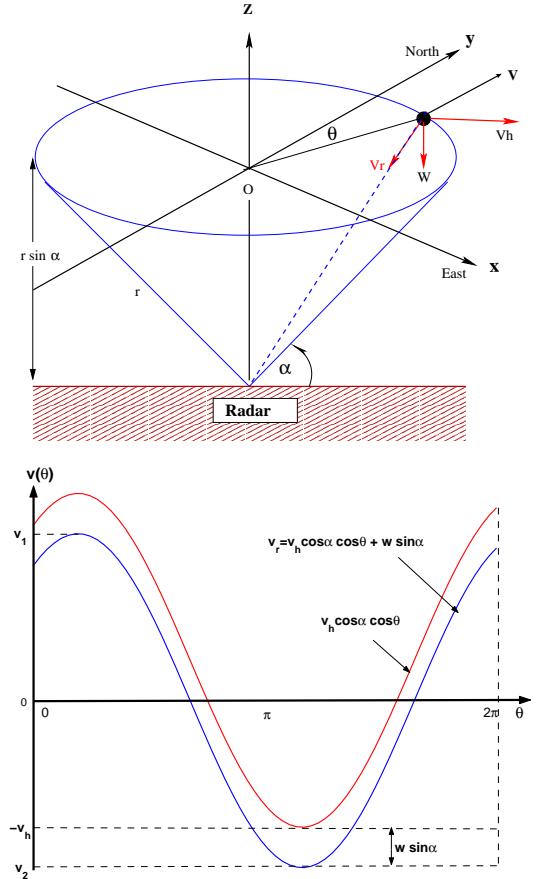


Figure 2. Geometry for scan of velocities on a Velocity Azimuth Display (VAD) circle (top) and the variation of the radial velocity deduced from horizontal and vertical (precipitation fall velocity) components (bottom).

The simplest case is to consider a horizontally uniform wind field for both, horizontal and vertical (precipitation fall velocity) components. In such a case, if we make measurements of the velocity along circles centred at the radar by azimuthal scanning at a constant elevation angle (PPI), we get, for a constant distance from the radar, a sinusoidal dependency of the measured radial velocity on the azimuthal angle. Assuming that the horizontal wind velocity v_h and hydrometeor fall speed w are uniform over the area being observed, then the mean Doppler velocity

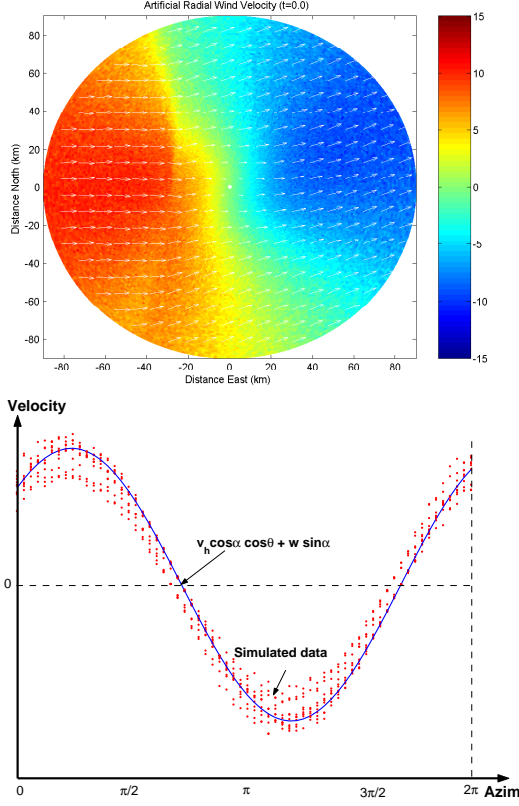


Figure 3. Artificial radial velocity with Gaussian noise (top), and the data for radial velocity (shown as dots) versus azimuth angle at 30km range (bottom). The solid line is the variation without any error.

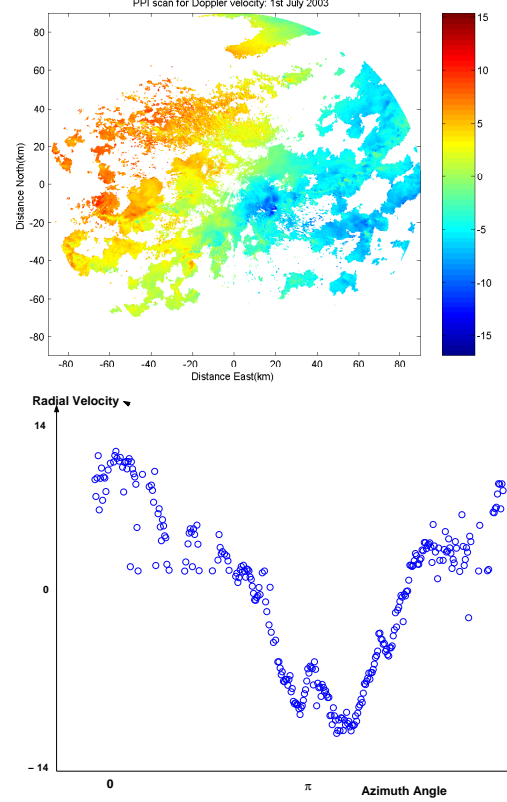


Figure 4. Observed Doppler radial winds on 1st July 2003 from Chilbolton radar (top), and the data displaying as radial velocity versus azimuth angle at a particle range, at 30km (bottom).

\bar{v}_r varied sinusoidally with maxima and minima occurring when the beam azimuth passes the upwind ($\theta = 0$) and downwind ($\theta = \pi$) directions, that is when

$$\begin{aligned} v_{r1} &= v_h \cos \alpha + w \sin \alpha, & \text{when } \theta = 0, \\ v_{r2} &= -v_h \cos \alpha + w \sin \alpha, & \text{when } \theta = \pi. \end{aligned} \quad (1)$$

Hence

$$v_h = \frac{v_{r1} - v_{r2}}{2 \cos \theta}, \quad w = \frac{v_{r1} + v_{r2}}{2 \sin \theta}. \quad (2)$$

Then the horizontal divergence is given by the formula

$$\text{div} v_h = \frac{1}{\pi R \cos \theta} \int_0^{2\pi} v_r d\theta - \frac{2w \tan \theta}{R}, \quad (3)$$

where R is the radius of the radar sampling circle at height l . However, Eq. (3) is only valid for low elevation angles.

Using the formula

$$v_r = u \sin \theta \cos \alpha + v \cos \theta \cos \alpha + w \sin \alpha \quad (4)$$

to derive the wind velocity, we compare a plot derived from Fig. 3(top) with a perfect *sine wave* displayed in Figure 3(bottom). The impact of the simulated errors is to cause the differences between the data (dots) and the no error sine curve (solid line) shown. Figure 4(top) displays a real data case for the PPI scan from the Chilbolton radar on 1st July 2003, and Figure 4(bottom) shows the radial velocity versus azimuth angle from the observed data shown. The deviation from a perfect *sine wave* shown in Figure 4(bottom) relates to a combination of the impact of measurement and instrumental errors, and the vertical variation of wind velocity with height caused by both the boundary layer turbulence and synoptic scale motions. It is possible to use the simulator

to investigate, in more detail, the impact of various errors on the radial winds. This is the subject of continuing study.

3. 3D-Var data assimilation

Data assimilation, into a mesoscale NWP model, may use a variational approach to retrieve three dimensional cloud and wind fields from radar observations of radial velocity from single radar inside the analysis domain. This variational analysis system uses also satellite data and surface data observations. The 3D-Var systems implement an incremental formulation (for a review see, for example, [20]). Under the assumption that the background and observation errors are Gaussian, random and independent of each other, the *optimal* estimate $\mathbf{x}_a = \mathbf{x}_b + \delta\mathbf{x}$ in the analysis space is given by the incremental cost function

$$\mathcal{J}[\delta\mathbf{x}] = \frac{1}{2}\delta\mathbf{x}^T\mathbf{B}^{-1}\delta\mathbf{x} + \frac{1}{2}[\mathbf{H}\delta\mathbf{x} - \mathbf{y} + \mathcal{H}\mathbf{x}_b]^T\mathbf{E}^{-1}[\mathbf{H}\delta\mathbf{x} - \mathbf{y} + \mathcal{H}\mathbf{x}_b] \quad (5)$$

where $\delta\mathbf{x} \equiv \mathbf{x}_a - \mathbf{x}_b$ is the state vector of the analysis increments (the estimated variable is then given by $\mathcal{H}\mathbf{x}_b + \mathcal{H}\delta\mathbf{x}$), \mathbf{x}_b is the state variable of the background of \mathbf{x} that includes the radial wind variable, and \mathbf{y} is the observed vector that includes the observed radial winds in the observation space. \mathcal{H} is the nonlinear observation operator that relates the model variables to the observation variable and a transformation between the different grid meshes, and \mathbf{H} is the *linear* observation operator with elements $h_{ij} = \partial\mathcal{H}_i/\partial x_j$. \mathbf{B} is the background covariance matrix and \mathbf{E} is a diagonal matrix of the error covariance in the observations, and in the observation operator (see [13]). Miller and Sun [17], and Xu and Gong [25] assumed that the observation error covariance matrix \mathbf{E} is diagonal with constant diagonal elements given by the estimated observation error, which was taken as 1 m/s for typical radar observations. We provide later in this paper a different approach to the representation of the errors of observed radial winds.

To avoid the computationally overwhelming problem of inverting the covariance matrix \mathbf{B} in the minimization of the cost function (5), and to accelerate the convergence of the minimization algorithm, a pre-conditioning of the minimization problem is needed (see [13]). This can be achieved by defining a variable \mathbf{U} to be applied to the assimilation increment $\delta\mathbf{x}$ ($\mathbf{U}\delta\mathbf{x} \equiv \mathcal{X}$) such that it transforms the

forecast error ϵ in the model space into $\tilde{\epsilon}$, a variable of an *identity* covariance matrix (i.e., $\langle \tilde{\epsilon}, \tilde{\epsilon}^T \rangle = \mathbf{I}$, where $\langle \cdot, \cdot \rangle$ is an inner product). This change of variable can be written as $\epsilon = \mathbf{U}^{-1}\tilde{\epsilon}$. Thus

$$\mathbf{B} = \langle \epsilon, \epsilon \rangle = \mathbf{U}^{-1} \langle \tilde{\epsilon}, \tilde{\epsilon}^T \rangle \mathbf{U}^{-T}, \text{ or } \mathbf{B}^{-1} = \mathbf{U}^T \mathbf{U}. \quad (6)$$

This leads to a new representation of the incremental cost function of the form

$$\mathcal{J}[\mathcal{X}] = \frac{1}{2}\mathcal{X}^T\mathcal{X} + \frac{1}{2}[\mathbf{H}\mathbf{U}^{-1}\mathcal{X} - \mathbf{y} + \mathcal{H}\mathbf{x}_b]^T\mathbf{E}^{-1}[\mathbf{H}\mathbf{U}^{-1}\mathcal{X} - \mathbf{y} + \mathcal{H}\mathbf{x}_b] \quad (7)$$

With this cost function, no inversion of \mathbf{B} is needed. The control variables \mathcal{X} are horizontal and vertical wind components, potential temperature, density, pressure and specific humidity. Here, we assume that the matrix \mathbf{E} includes the errors from the *observations* (original measurements), *observation operator*, and *super-obbing procedure*³. The 3D-Var analysis is then performed using continuous cycling procedure. The length of the assimilation window in each analysis is determined according to the model resolution. In each analysis cycle, the optimal analysis is obtained by minimizing the cost function (7) using iterative procedure.

The matrix \mathbf{U}^{-1} in (7) may be realized as

$$\mathbf{U}^{-1} = D\mathbf{F}, \quad (8)$$

where D is a diagonal matrix of standard deviation of the background error specified by the error estimation of numerical experiments, and F is the square root of a matrix whose diagonal elements are equal to one, and off-diagonal elements are the background error correlation coefficients. In practical data assimilation for NWP, the full matrix F is too large to compute explicitly or store into computer memory. Assumptions and approximations are made such that the effect of F on the control variable \mathcal{X} in Eq. (7) is achieved through the use of equivalent spatial filter; see the work of Purser and McQuigg [19], Lorenc [14], and Hayden and Purser [7], for further details.

In the next two sections we explain how to preprocess data to make it suitable for the variational assimilation system.

³*Super-obbing procedure* is a technique to combine (re-scale) the radar observations, using statistical interpolation, at a larger spatial scale which is compatible with the model; see §4.2.

4. Pre-processing of Doppler Radial Wind data

4.1. Quality control

The major steps in processing the data before the assimilation are interpolation of data from/to a Cartesian grid, removing the noisy data, and filtering. Data *quality control* (QC) is a technique, which should be performed for each scan, to remove undesired radar echoes, such as ground clutter and anomalously propagated clutter (AP clutter), sea clutter, velocity folding, and noise using the threshold, that any velocity data with values less than, say, 0.25 m/s and their corresponding reflectivity are removed. Unfolded Doppler velocity, in Chilbolton radar, are measured using both horizontally and vertically polarised pulses. This parameter is the component of the target velocity towards the radar (positive velocities are towards the radar). Noise are removed on the basis of the variance of the velocity at each pixel with its neighbours, which can occasionally remove good data with genuinely high variance.

The data QC should also be designed to correct the errors in the observed radial winds, $v_r^{(0)}$, caused by velocity folding and velocity aliasing, using the Nyquist velocity, v_{nyq} , and model background velocity, $v^{(b)} = (u^{(b)}, v^{(b)}, w^{(b)})$. The process may involve:

1. Interpolating from model grid to observation points, calculating the background radial velocity $v_r^{(b)}$ and then estimate the difference

$$v_r^{(d)} = v_r^{(0)} - v_r^{(b)};$$

2. Taking the integer part n from $v_r^{(d)}/(2v_{nyq})$ and adjusting the observational radial velocity to

$$v_r = v_r^{(0)} - 2nv_{nyq};$$

3. If the absolute value of the adjusted radial velocity v_r is less than $0.5v_{nyq}$, then it is a "good" one estimate. Otherwise, we check by comparing this value with the "good" values at the surrounding points and keeping (or rejecting) this value if the difference is larger than (say) 3 m/s.

A final quality check is made to remove any remaining spurious data by computing the local standard deviation (SD) of each data point from its local mean. Data with large SD being given small weight or discarded; see [23].

4.2. Super-obbing radial wind data

Doppler radars produce raw radial wind data with high temporal and spatial density. The horizontal resolution of the data is around 300m (that is too high to be used in the assimilation scheme) whereas the typical resolution of an operational mesoscale NWP model is of the order of several kilometers. To reduce the representativeness error, and correspond the observations to the horizontal model resolution, one may use spatial averages of the raw data, called *super-observations*. The desired resolution for the super-observations can be generated by defining parameters (which can be freely chosen) for the range spacing and the angle between the output azimuth gates.

As we have mentioned previously, a direct assimilation of PPI data with no vertical interpolation is recommended. Moreover assimilation using radar data directly at observation locations avoids interpolation from an irregular radar coordinate system to a regular Cartesian system, which can often be a source of error especially in the presence of data voids (see [20]). We have developed a software package, which is based on spatial interpolation in polar space, for processing of raw volume data of radial velocity in PPI format to super-obbb the data to the required resolutions for the 3D-Var system in the Met Office. Figure 5 provides an example of super-observations generated through averaging the raw data at 4km resolutions along the radar beam, and 1 degree azimuth resolution.

Since the super-obbing procedure is based on statistical interpolation, the expected error of the super-obbing procedure is regarded as the observation error of the super-observations. It is desirable that the error of super-observations is uncorrelated with the background error. Representativeness error for the superobbing procedure error are accounted for by using the local standard deviation, which obviously increases with the range; see Figure 6.

5. A representation of errors for observation radial winds

In order to optimally assimilate Doppler radar radial velocity observations into NWP model, it is necessary to know their error covariances. We assume that the observational errors are uncorrelated in space and time. Under this assumption, the observation error covariance matrix Σ ($\equiv \mathbf{E}$) in the cost function (7) can be reduced to a diagonal matrix. Then the matrix \mathbf{E} , in Eq. (7), is regarded as a weighting coefficient that reflects the relative

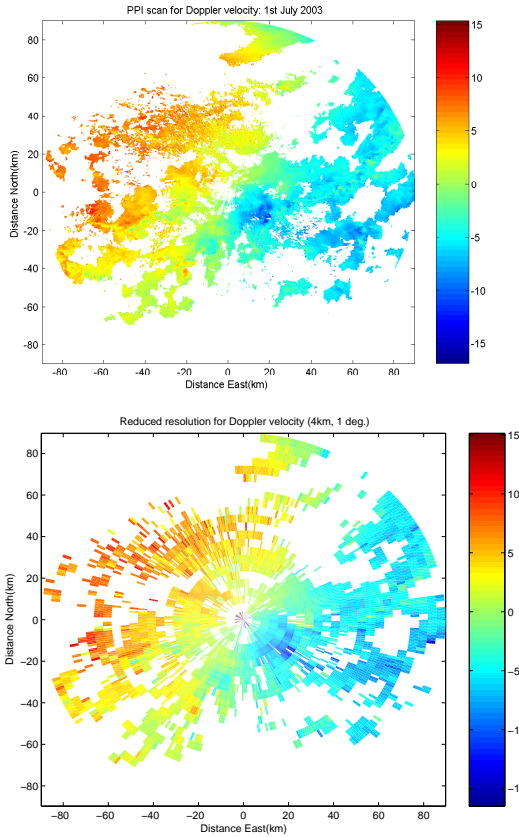


Figure 5. An example of the Doppler radar radial raw data (top) and the super-obbed Doppler radial winds (bottom) at $4km$ resolution along the radar beam and 1 degree azimuth angle resolution.

precision of the data (measurement uncertainty and representativeness error). The matrix Σ can be expressed as:

$$\Sigma = \text{diag}[\sigma^2(\varepsilon)], \quad (9)$$

where $\sigma^2(\varepsilon)$ is the error variance of the radial velocity v_r . The most common error in radar radial winds are (i) the noise in the radial velocity induced by the velocity gradient across the pulse volume with variance $\check{\sigma}^2(\varepsilon_v)$, and (ii) the instrumental error due to hardware degradation of variance $\hat{\sigma}^2(\varepsilon_i)$. Miller and Sun [17] state that these measurement errors need to be specified so that radar observations can be properly assimilated for NWP. However, they note that the mean radial velocity and spectral width estimators are proportional to the radar wavelength and the time spectral width [4], and therefore are rather impractical as estimates of the measurement errors. They therefore note a need for error estimators of

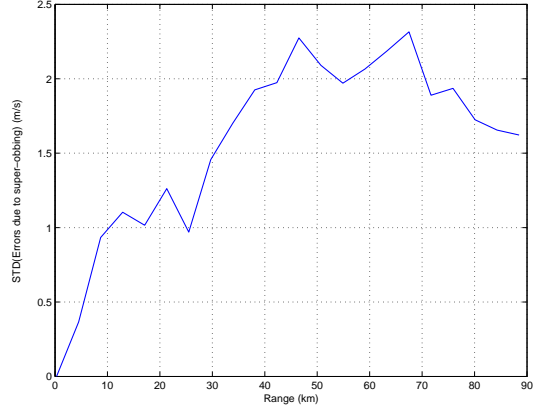


Figure 6. Local super-observation error standard deviation at $4km$ resolution.

radial velocity that can be obtained from the measurements themselves.

5.1. Error due to the velocity gradient within and across the pulse volume

The local sampling of the radial velocity is employed to approximate the error variance $\check{\sigma}_{v_r}^2$, since noisy data are usually associated with high values of radial velocity variance.

Errors in the original measurements of the radial velocity within each radar pulse volume depend on the strength of the returned signal and the spread (or width) of the Doppler velocity spectrum that depends on the velocity gradients. Since the radar scatterers in the pulse volume move randomly, we assume that the errors of the velocity gradient of the radar backscatterers are given by a normal (Gaussian) distribution, where,

$$pdf(\varepsilon_v) = \int_{-\infty}^{\infty} \frac{1}{\sqrt{2\pi}\check{\sigma}} e^{-\varepsilon_v/2\check{\sigma}^2} d\varepsilon_v. \quad (10)$$

The error variance $\check{\sigma}^2$ is modified by the velocity gradient (which varies with time) along the pulse volume. The variations of this velocity difference along the pulse volume cause the kinetic energy (KE) of the moving scatterers to change. We will assume here for simplicity that this velocity difference is taken in the radial direction only. Here,

$$\text{the rate of change in the KE} = \mathcal{F}\Delta v_r, \quad (11)$$

where \mathcal{F} is an arbitrary force applied to the scatterers and Δv_r is the velocity difference along the pulse volume. Thus the increase in the kinetic energy in time interval dt , during which the scatterer moves a

distance dr , is

$$d(KE) = dW, \quad (12)$$

where dW is the work done by the force \mathcal{F} in the infinitesimal displacement dr taken as the pulse length and over time dt .

Rogers and Trips [21] show that the change in the kinetic energy per unit mass can be expressed as

$$d(KE) = \sigma^2(v_r), \quad (13)$$

where $\sigma^2(v_r)$ is the variance of the mean Doppler velocity, which can be expressed by (see [4])

$$\sigma^2(v_r) = \frac{\lambda}{8\sqrt{\pi}MT}\varphi, \quad (14)$$

where λ is the radar wavelength, φ is the true spectral width, M is the number of equally spaced pulses, and T is the time between pulses. (The maximum unambiguous (Nyquist) velocity is $v_{nyq} = \lambda/4T$.)

Nastom [18] investigated the factors impacting on the spectral width of Doppler radar measurements. For very small bandwidths it was found that the variance was dominated by the effects of wind speed changes along the radar beam. The expression for the variance was derived as a function of the beam elevation and the vertical wind shear. We therefore chose here to express the error variance $\check{\sigma}^2(\varepsilon_v)$ of radial winds more simply in terms of the gradient variance along the pulse volume in a radial direction as follows

$$\check{\sigma}^2(\varepsilon_v) = \left(1 - e^{-|\Delta v_r/v_r|}\right) \sigma^2(v_r), \quad (15)$$

where Δv_r is the gradient of the radial velocity, measured as a centred difference across the pulse volume. The error in radar radial winds due to the velocity gradient along the pulse volume varies with the range R . Figure 7 (top) displays the local radial velocity errors ($m \text{ sec}^{-1}$) calculated using (15) for the case of 1st July 2003, shown in Figure 4(top). Figure 7(bottom) shows a proposed s-function for the observation errors as a function of the range, which is acceptable to represent the errors of the radial velocity. Note that as the range increases the error increases. This is to be expected as the radar beam gets wider and the pulse volume greater the kinetic energy variation of the scatters in the pulse volume increases, with increasing range.

5.2. Error due to hardware degradation

Although the instrumental error can have a significant impact on the retrieval, in practice it is difficult to determine how this error varies with time.

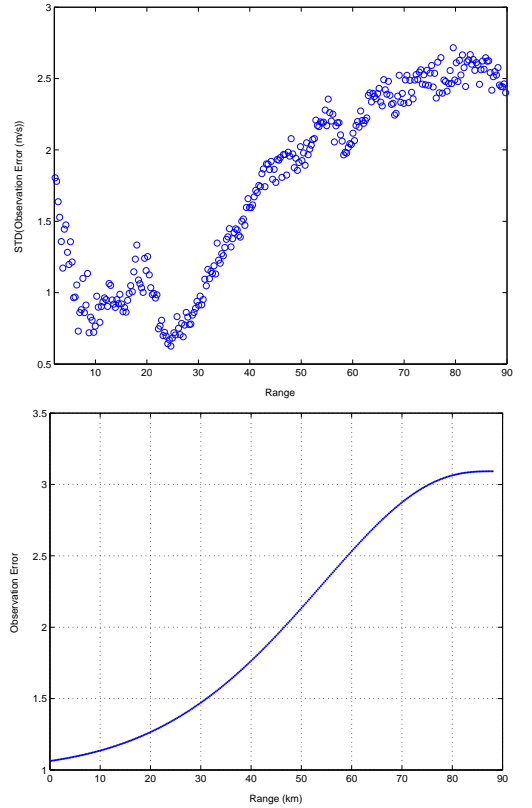


Figure 7. Local errors (m/sec) of the observation radial velocity for the 1st July 2003 case (top), and the proposed s-function for the observation errors as a function of the range (bottom). The errors are measured over all azimuths for each range. We can see the variability of the error increases as the range increases.

In this case we assume that the instrumental error does not vary temporally, and take the instrumental error variance as $\hat{\sigma}^2(\varepsilon_i)$ assuming there is no hardware degradation with time. Therefore the total error variance of the radial winds is given by

$$\begin{aligned} \sigma^2(\varepsilon) &= \check{\sigma}^2(\varepsilon_v) + \hat{\sigma}^2(\varepsilon_i) \\ &= \left(1 - e^{-|\Delta v_r/v_r|}\right) \sigma^2(v_r) + \hat{\sigma}^2(\varepsilon_i) \end{aligned} \quad (16)$$

at each (r, θ) . In the 3 – GHz Chilbolton radar, the measurement accuracy for Doppler radial velocity is about 0.15 – 0.5 m/s.

The instrumental error may not be a function of (r, θ) , but is a function of time. In this case, we assume that this error is represented by a "skewed" distribution such as a Chi-Squared distribution with probability density function (for ν degrees of free-

dom) given by

$$pdf_{\nu}(\varepsilon_i) = \frac{\varepsilon_i^{(\nu-2)/2} e^{-\varepsilon_i/2}}{2^{\nu/2} \Gamma(\nu/2)}, \quad \text{for } \varepsilon_i \in [0, \infty). \quad (17)$$

Here $\Gamma(y)$ is the *gamma function*, and ε_i is considered as the instrumental error.

Thus the error variance of the degradation is defined by

$$\hat{\sigma}^2(\varepsilon_i) = \int pdf_{\nu}(\varepsilon_i) (\varepsilon_i - \bar{\varepsilon}_i)^2 d\varepsilon_i, \quad (18)$$

where $\bar{\varepsilon}_i$ is the mean value of the instrumental error.

6. Direct assimilation and observation operator of PPI data

Due to the poor vertical resolution of radar data, a vertical interpolation of radar data from constant elevation levels to model Cartesian levels can result in large errors. For this reason a direct assimilation of PPI data with no vertical interpolation was recommended in [22,23]. However, radar data has better horizontal resolution than that of the model (the poorest polar radar data is approximately 0.5 km at the farthest range distance). An observation operator must be formulated to map the model variables from model grid into the observation locations such that the distance between the observations and model solution is estimated in the *cost function*. Thus, we take advantage of the vertical resolution of the model being much better than those of radar data. The observation operation, \mathcal{H}_e , for mapping (and averaging) the data from the model vertical levels to the elevation angle levels is formulated as

$$v_{r,e} = \mathcal{H}_e(v_r) = \frac{\sum G v_r \Delta z}{\sum G \Delta z}, \quad (19)$$

where $v_{r,e}$ is the radial velocity on an elevation angle level, v_r is the model radial velocity, and Δz is the model vertical grid spacing. The function $G = e^{-\alpha^2/2\beta^2}$ represents the power gain of the radar beam, β (in radians) is the beam half-width and α is the distance from the centre of radar beam (in radians). The summation is over the model grid points that lie in a radar beam.

We next discuss the observation operator to convert the Cartesian model components to the radial components.

6.1. Observation operator

There are two types of *observation operators*. One is used to interpolate and transfer the radar data from observation locations to the model grids. The

second is used to map the model data into the observation locations. In the case of a direct assimilation of *radar radial wind* at constant elevation angles, which is not a model variable, the *observation operator* involves: (i) a bilinear interpolation of the NWP model horizontal and vertical wind components u , v and w to the observation location; (ii) a projection of the interpolated NWP model horizontal wind, at the point of measurement, towards the radar beam using the formula

$$v_h = u \sin \theta + v \cos \theta, \quad (20)$$

where θ is the *azimuth* angle (clockwise from due North).

The elevation angle should include a correction which takes account of earth surface curvature and radar beam refraction (see [12]); Then the third step (iii) involves the projection of v_h in the slantwise direction of the radar beam as

$$v_r = v_h \cos(\alpha + \phi) + w \sin(\alpha + \phi), \quad (21)$$

$$\phi = \tan^{-1} \left(\frac{r \cos \alpha}{r \sin \alpha + d + h} \right), \quad (22)$$

where α is the *elevation* angle of the radar beam. The formula for ϕ represents approximately the curvature of the Earth. In the term ϕ , r is the range of observation, d is the effective radius of the Earth and h is the height of the radar above the sea level. The effective earth radius is 1.3 times the actual earth radius, this compensates for radar beam refraction. Note that the factor of 1.3 is valid only in the case of a standard atmosphere profile. The factor actually varies according to atmospheric conditions and should ideally be calculated from the variation of refractive index with height (see [12]). The effect of this correction term on results is very small.

7. Impact of assimilation of Doppler radial winds

In this section we investigate the impact of assimilation of radial velocity on the variational analysis and on the model forecasts. An experiment with 3D-Var has been performed at 12km and 4km resolution, using the Chilbolton radial winds PPI scan data for the 12z 1st July 2003 case. The raw data was averaged to about 4km resolution and estimated observational errors assigned. The size of the RMS errors assigned was a function of observation range and the error magnitude was of order $2 - 6m/s$, values which are similar to the errors in the radar winds discussed in the reviewer carried out in the EU COST

75 project [2]. There is a fair degree of arbitrariness in the error magnitude, as the theoretical model (see Figure 7) only predicts the shape of the error distribution. It was found that errors of this magnitude did not cause excessive degradation in the fit of the Var analysis to the other observation types assimilated along with radial winds.

In each Var experiment analyses were generated using *surface*, *aircraft* and *sonde observations* (and also *satwinds* in the 4km experiments), both with and without radial winds observations. Combination of radial winds (and their errors) and other input data can interact to produce non-linear results. However, in the case studied the initial experiments indicated that the radial winds do seem to produce a significant impact on the analysis. Figure 8 (with 12km resolution), and Figure 9 (with 4km resolution) show the impact of the Chilbolton radial winds on the NWP analysis. The top panel shows wind speed analysis without radial winds (computed from the analysed u and v increment fields) at level 5 (700-800m height which is about half the height of the radar beam at its maximum range of 90km) for the case of 12 : 00 UTC on 1st July 2003. The middle panel is the analysis when radar radial data have been added to the other source of observations, and the bottom panel is difference between the two analysis, to show the contribution of the radial winds observations to the analysis. Note that the impact of using radial winds is confined to the vicinity of the coverage of the Chilbolton radar located in central southern England.

Our experiments indicate that it is possible to assimilate the super-obbed Doppler radar radial observations in PPI format into mesoscale NWP model, where the model counterpart is calculated by the observation operator discussed in §6.1. However, the results depend very strongly on the observation errors that may vary with the range.

Atmospheric model forecasts for the speeds at $T+3$ ($\equiv 15UTC$), and $T+6$ ($\equiv 18UTC$), level 5 from 12UTC on 1st July 2003 are displayed in Figure 10. Radial winds appears to have significant impact in both the variational analysis providing the model initialization, and then on the model forecasts. Indeed, the impact at $T+6$ is larger over South East England than at $T+3$. This consistent with the subsequent development of the line convection which occurred over South England on this day.

8. Conclusions

The mesoscale 3D-Var system has been developed in the Met Office to include the capability of assimilation of Doppler radial velocities. This paper have concerned particularly with the statistical errors of the radial wind data, the pre-processing of the data before assimilation that includes manual data quality control, and super-obbing the very high resolution raw data to match the model resolutions. The observation operator for the Doppler radial velocity has also been developed and incorporated in the VAR system. Examples of radial winds derived from the Chilbolton radar and a simulation model have been considered. The impact of the Doppler radial winds and their errors on the variational assimilation system and on the model forecasts have been investigated.

The Met Office 3D-Var system has been run with (and without) Doppler radial velocities (in PPI format) with 12km, and 4km model resolution. The Met Office Unified Model has also been run with the obtained initializations having a time window of 3 hrs. A mathematical representation of observation errors for radial winds has been used, and the form of representation has been tested. The S-curve representation seems to be appropriate, and consistent with the observations for the particular case studied. The numerical experiments led to a significant impact on the variational analysis and on the forecasts.

A considerable amount of effort is still required to further improve the system and to extend the experiments to assimilate 1-5km resolution gridded radial velocity and reflectivity data, using 4D-Var technique to produces initial/boundary conditions for 1-4km resolution forecasts.

Acknowledgements

This work represented in this paper is sponsored by the National Environmental Research Council (NERC) through the Universities Weather Research Network (UWERN), a part of the NERC Centres for Atmospheric Science (NCAS). The authors thank Dr Sean Swarbrick (Met Office) for his contribution in some parts of the paper and his valuable comments.

REFERENCES

1. Benjamin, S.G., Dévényi, D., Weygondt, S., Brundage, K.J., Brown, J.M., Grell, G.A., Kim, D., Schwartz, B.E., Smirnova, T.G., Smith, T.L. and Monikin, G.S. (2004): An hourly assimilation present cycle: The RUC, *Mon. Wea. Rev.*,

- 132**, 494–518.
2. Collier, C.G. (Editor) (2001): COST-75, Project, Advanced Weather Radar Systems 1993–199, European Commission EUR 19546, Brussels, 362pp
 3. Collier, C.G. (1996): Application of Weather Radar Systems. A guide to Uses of Radar Data in Meteorology and Hydrology, 2nd Edition, Wiley-Praxis, Chichester, 390pp.
 4. Doviak, J.D. and Zrnic, D.S. (1993): Doppler Radar Weather Observations, 2nd Edition, Academic Press, London/San Diego.
 5. Golding, B.W. (1999): Quantitative precipitation and forecasting in UK, *J. Hydrology*, **39**, 286–305.
 6. Gong, J. Wang, L. and Xu, Q. (2003): A three step dealiasing method for Doppler velocity data quality control, *J. Atmos. Ocean. Tech.*, **20**, 1738–1748.
 7. Hayden, C. M., and Purser, R.J. (1995): Recursive filter for objective analysis of meteorological fields: Applications to NESDIS operational processing. *J. Appl. Meteor.*, **34**, 315.
 8. Keeler, R.J. and Ellis, S.M. (2000): Observational error covariance matrices for radar data assimilation, *Phys. Chem. Earth (B)*, **25**, 1277–1280.
 9. Kibble, T.W.B (1966): Classical Mechanics, McGraw-Hill, London, 296 pp.
 10. Krzysztofowicz, R., and Collier, C.G. (Editors) (2004): Quantitative Precipitation Forecasting II. Special Issue of *J. Hydrology*, **288** nos 1–2, 236pp.
 11. Lin, Y., Ray, P.S., and Johnson, K.W. (1993): Initialization for a modeled convective storm using Doppler radar data-derived fields. *Mon. Wea. Rev.*, **124**, 1757–2775.
 12. Lindskog, M., Salonen K., J?rvinen, H. and Michelson, D. B., (2004): Doppler radar wind data assimilation with HIRLAM 3D-Var. *Monthly Weather Review*, **132**, p1081.
 13. Lorenc, A.C. (1997): Development of an operational variational scheme, *J. Meteorol. Soc. Japan*, **75**, 339–346.
 14. Lorenc, A.C (1992): Iterative analysis using covariance functions and filters. *Quart. J. Roy. Meteor. Soc.*, **118**, 569591.
 15. Macpherson, B., Wright, B.J., Ward, W.H. and Maycork, A.J. (1996): The impact of MOPS moisture data in the UK Meteorological Office mesoscale data assimilation scheme. *Mon. Wea. Rev.* **124**, 1746–1766.
 16. May, P.T., Sato, T., Yamamoto, M., Kato, S., Tsuda, T. and Fakao, S. (1989): Errors in the determination of wind speed by Doppler radar. *J. Atm. Ocen. Tech.*, **6**, 235–242.
 17. Miller, L.J. and Sun, J. (2003): Initialization and forecasting of thundstorms: specification of radar measurement errors. *31th conf. on Radar Meteorology*. Amer. Meteor. Soc., Seattle, Washington. pp 146–149.
 18. Nastrom G.D. (1997): Doppler radar spectral width broadening due to beamwidth and wind shear, *Ann. Geophysicae*, **15**, 786–796.
 19. Purser, R. J., and McQuigg, R. (1982): A successive correction analysis scheme using numerical filter. Met Office Tech. Note **154**, 17 pp.
 20. Rihan, F.A., Collier, C.G., and Roulstone, I. (2005): Four-Dimensional Variational Data Assimilation for Doppler Radar Wind Data, *J. Comput. Appl. Math.* **176**(1) 15–34.
 21. Rogers, R.R., and Trips, B.R. (1964): Some radar measurements of turbulence in snow, *J. Appl. Meteor.*, **3**, 603–610.
 22. Sun, J. and Crook, N.A. (2001): Real-time low-level wind and temperature analysis using single WSR-88D data. *Wea. Forecasting*, **16**, 117–132.
 23. Sun, J. and Crook, N.A. (1998): Dynamical and microphysical retrieval from Doppler radar observations using a cloud model and its adjoint. Part II: retrieval experiments of an observed Florida convective storm. *J. Atmos. Sci.*, **55**, 835–852.
 24. Sun, J. and Crook, N.A. (1997): Dynamical and microphysical retrieval from Doppler radar observations using a cloud model and its adjoint. Part I: Model development and simulated data experiments. *J. Atmos. Sci.*, **54**, 1642–1661.
 25. Xu, Q. and Gong, J. (2003): Background error covariance functions for Doppler radial wind analysis. *Q.J. R. Meteorol. Soc.*, **129**, 1703–1720.

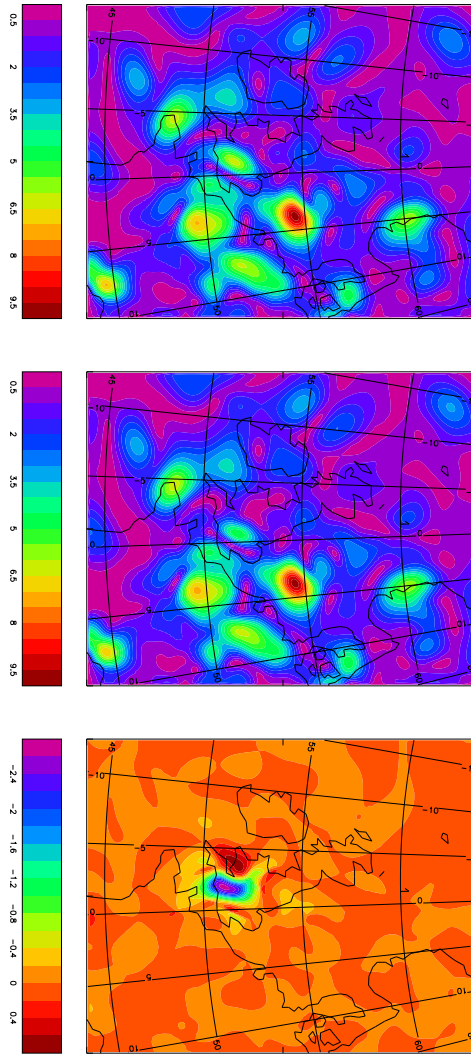


Figure 8. Impact of the radar radial winds on the 3D-Var analysis with 12km model resolution for the wind speed at level 5, for 12UTC 1st July 2003. From top to bottom: the PFAnalysis without radial winds, with radial winds, and the difference.

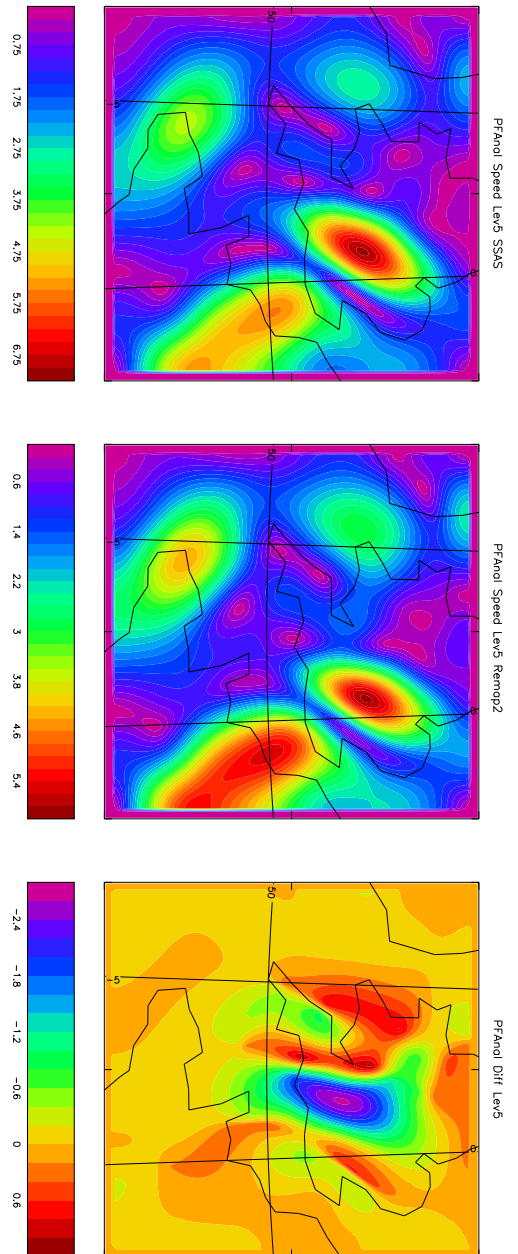


Figure 9. Impact of the radar radial winds on the 3D-Var analysis with 4km model resolution at level 5, for 12UTC 1st July 2003. From top to bottom: the PF-Analysis without radial winds, with radial winds, and the difference.

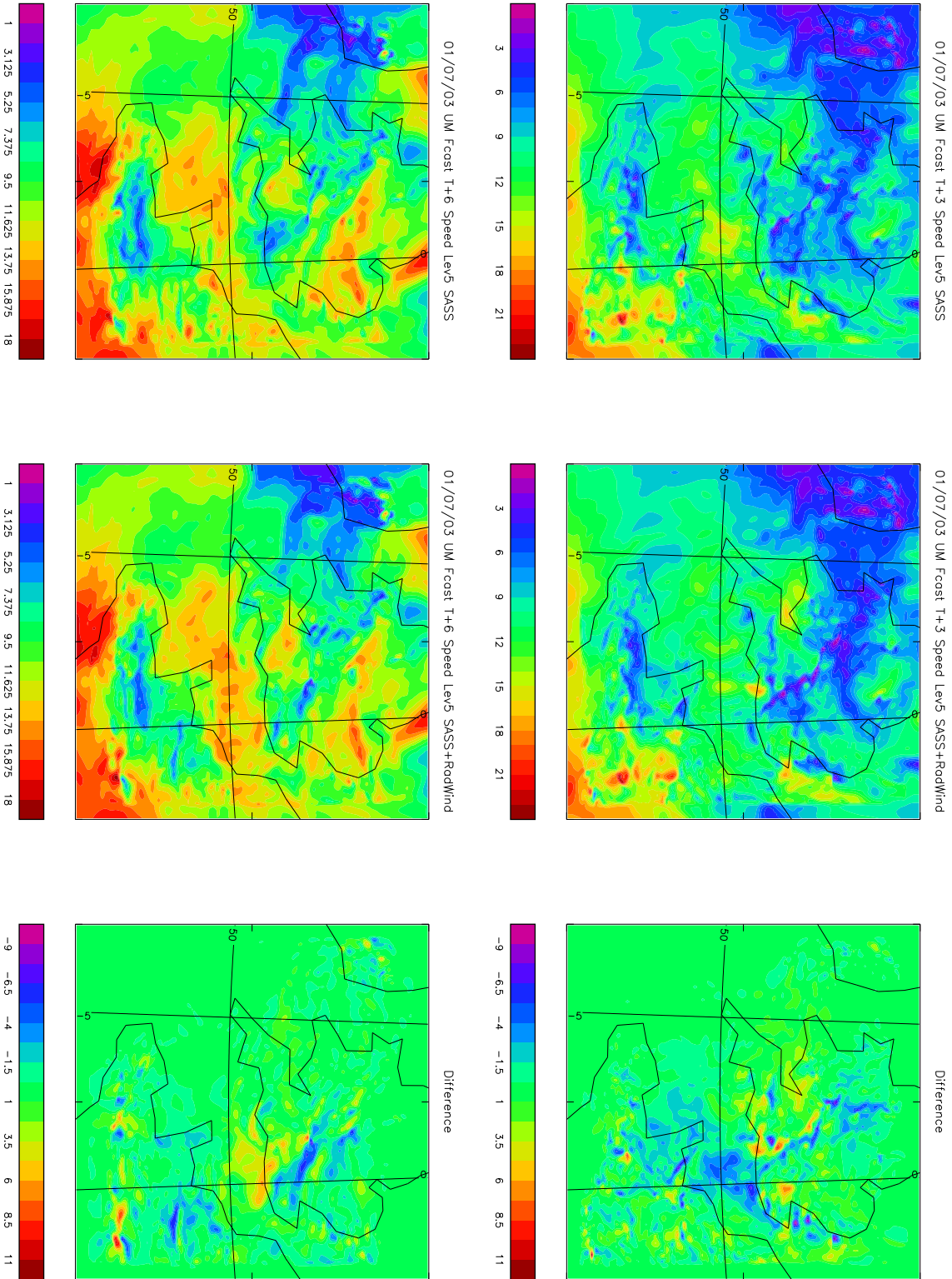


Figure 10. Atmospheric wind speeds at $T + 3$ (right) & $(T+6)$ (left), level 5 from 12UTC on 1st July 2003. From top to bottom: the forecast without radial winds, with radial winds, and the difference.